

## A NUMERICAL SIMULATION VALIDATION STUDY: HIGH-VELOCITY BLUNT PROJECTILE IMPACTS ON 2024-T351 ALUMINUM ALLOY PLATES OF VARYING THICKNESSES

Mohd Zaid Othman<sup>a\*</sup>, Tan Kean Sheng<sup>a</sup>, Amir Radzi Ab Ghani<sup>b</sup>

<sup>a</sup> Department of Mechanical Engineering, Faculty of Engineering, National Defence University of Malaysia, Sg. Besi Camp, 57000 Kuala Lumpur, Malaysia

<sup>b</sup> College of Engineering, MARA University of Technology (UiTM), 40450 Shah Alam, Selangor, Malaysia

### ARTICLE INFO

#### ARTICLE HISTORY

Received : 12-10-2024  
Revised : 16-12-2024  
Accepted : 04-03-2025  
Published : 31-05-2025

#### KEYWORDS

Ballistic  
Impact  
LS-DYNA  
Numerical Simulation  
Projectile

### ABSTRACT

In this current study, a numerical simulation approach is employed to investigate the post-impact behaviours of a blunt cylindrical projectile colliding with a fully clamped and bolted square plate made of 2024-T351 aluminium alloy. The plate has a circular perimeter with a diameter of 116 mm, and its top surface is oriented at a right angle to the incoming projectile. Various initial velocities are applied to rigid projectiles, which impact plates of thicknesses ranging from 2 mm to 8 mm, all made from 2024-T351 aluminium alloy. A total of forty-four numerical simulation analyses are conducted to study the impacts of blunt cylindrical projectiles on these aluminium alloy plates. The results show excellent agreement with an average difference of 15.04 % when compared to published experimental test data, validating the accuracy of the numerical simulations.

## 1.0 INTRODUCTION

Studies on protective structures against impact loadings are well established and published all around the world. Circular aluminium plates with geometrical imperfections impacted at low velocity had been investigated numerically and experimentally, in their paper they found out that intact plate was more tough for low velocity impact for stiffer types of materials [1-3]. The investigation of the performances of aluminium alloy plates against bullet impact at different velocities and thicknesses had been performed numerically, they observed that if a bullet's speed of 720 km/h hits a target plate, the target plate will experience total perforation even though the plates' thicknesses were increased [4-6]. Borvick et al [7] studied the effects of 90 degrees and angled impact of bullet against aluminium plate via the experimental and numerical simulation methodologies, they found out that the optimum angle of impact was 60 degrees where the bullet impact gradually changes from perforation to bouncing of bullet hit at 90 degrees and the angled target plate.

The mode of deformations of transparent armour against countless bullet hits had been studied experimentally [8-10], their study deduced that in the in-plane direction of the target plate, the failure of the target plate propagates in the outward directions from the impact central location due to the existence of circumferential failure that stopped the progression of radial failures. The failure of glass plates due to impact loadings have been studied numerically by utilizing the peridynamics approach [11-13], they observed that good agreements were produced between the coefficient of restitution and the model predictions. Yuan et al [14] investigated the dynamic performances of bullet impact against gelatine incorporated shield target to further understand the injuries towards the human bodies, they discovered that nearly 50.00 % of the kinetic energy was absorbed by the target shield while the other 50.00 % of the kinetic energy was absorbed by the gelatine. The study of three-dimensional printed layered plate against high-speed impact bullet had been performed by utilizing the numerical simulation and mathematical approaches [15-16], they observed that a layered sets of plates had managed to reduce the residual velocity of the bullet as compared to a single target plate of the same thickness. Elveli et al [17], investigated the

efficiencies of small projectiles impacting thin blast loaded steel plates, they observed that with the increase in the stiffness of the target plate, the overall failure reduced greatly, and the specific failure of an area surged. The effects of gravity induced bullet impact against human's skull have been studied by using the numerical simulations by Celik and Koc [18], they discovered that a bullet that falls freely under gravity could cause fatal injuries to human skull.

Among the important points that are presently being researched and had been investigated in the studies of projectiles impacts on target plates are the material properties of the projectile and target plate, the initial velocity of the projectile, the residual velocity of the projectile after impact, the geometrical shapes of the projectiles' heads, the cross sectional geometry of the projectile's body, the angle of impact of the projectile upon impacting the target plate, the thickness of the target plate, the layered thicknesses of the target plate and the pattern of deformation of the target plate upon impact. Experimental tests that required advanced apparatus, analytical formulations to predict certain outputs of the impact scenarios and numerical simulations that can modelled the projectile and target plate in three-dimensional degree of freedoms could be utilized to study the phenomena of projectile impact on a target plate. Numerical simulation analysis of blunt cylindrical projectile against the 2024-T351 aluminium alloy plate was employed in this study to acquire the predicted residual velocities and the predicted the patterns of deformations of the target plate due to its superiority in providing various predictions of outputs in three-dimensional degree of freedoms. Experimental tests data of blunt cylindrical projectile against the 2024-T351 aluminium alloy plate from published paper [19-20] will be used to validate the predicted numerical simulations analyses to maintain and preserve the accuracy of the predictions.

## 2.0 NUMERICAL SIMULATION METHODOLOGY

This section describes the steps taken to model the impact phenomena of the blunt cylindrical projectile against the 2024-T351 aluminium alloy plate by using the LS-PREPOST and LS-DYNA numerical simulation software. Before the numerical simulation steps are described in great detail, a published work on experimental test of a high speed impact of blunt cylindrical projectile against aluminium alloy plate [19] was selected for this validation study and will be fully described and utilized in this paper as a reference or as a case study in order to get a better understanding of the components that will be modelled and analysed in the numerical simulation analysis validation process. Once the blunt projectile and aluminium plate had been successfully modelled and analysed in LS-PREPOST and LS-DYNA numerical simulation software, the experimental tests data from the published work [19] will be used to validate on the accuracy of the numerical simulation predictions after it has been processed by LS-DYNA. Figure 1 shows a one stage gas gun [19] that was utilized to launch the blunt cylindrical projectile impacting against the 2024-T351 aluminium alloy plate; the gas system consists of a pressurized chamber, a launch tube, a laser velocity meter, an impact chamber, a blunt cylindrical projectile, a 2024-T351 aluminium alloy plate as the target plate and a high speed camera. The laser velocity measured the initial velocity of the blunt cylindrical projectile; the initial velocity of the gas gun can be varied by varying the gas in the pressurized chamber. After the blunt cylindrical projectile impacted and perforated the 2024-T351 aluminium alloy plate, the velocity that passed the target plate was known as the residual velocity and the magnitude of the residual velocity was measured by the high-speed camera.

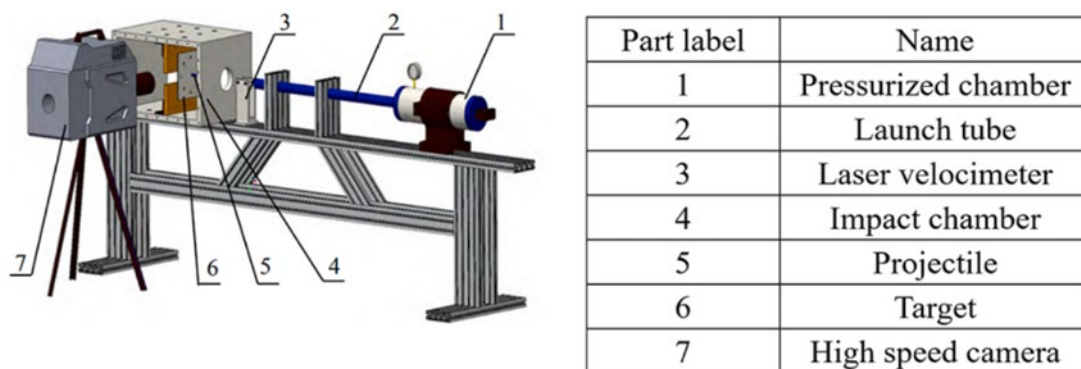


Figure 1. Experimental setup of the high-speed impact of blunt projectile against 2024-T351 aluminium alloy plates [19]

The 2024-T351 aluminium alloy plate that was used in the experimental tests was made of 130.00 mm x 130.00 mm square geometry with four different thicknesses i.e. 2.00 mm, 4.00 mm, 4.82 mm and 8 mm in Figure 2. The 2024-T351 aluminium alloy plate was clamped in between two steel frames by using 12 units x 6.00 mm in diameter bolts around its circumferential exposing an area of 116 mm diameter circular plate. Only one type of rigid blunt cylindrical projectile was utilized in the experimental tests performed i.e. 12.66 mm in diameter x 50.66 mm in height as in Figure 2 and Table 2. The rigid blunt cylindrical projectile was launched by the pressurized chamber and the launch tube in Figure 1; impacted the 2024-T351 aluminium alloy plate at the central location of the circular plate at a right-angle direction to the surface of the target plate. Table 1 shows a total of 44 number of experimental impact tests performed on the four different thicknesses of the target plate. The first test consisted of 12 A-series i.e. 12 different initial velocities of the rigid blunt cylindrical projectile impacted against a 2 mm target plate, the second test consisted of 9 B-series i.e. 9 different initial velocities of the rigid blunt cylindrical projectile impacted against a 4 mm target plate, the third test consisted of 11 B-series i.e. 11 different initial velocities of the rigid blunt cylindrical projectile impacted against a 4.28 mm target plate and finally the fourth test consisted of 12 A-series i.e. 12 different initial velocities of the rigid blunt cylindrical projectile impacted against a 8.00 mm target plate. All 44 numbers of experimental impact tests' residual velocities and their respective mode of deformations were recorded and will be utilized for the numerical simulation validation process in this section.

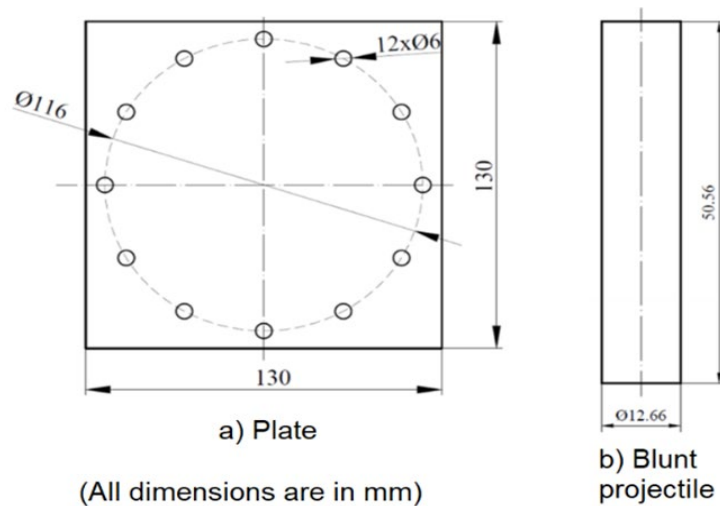


Figure 2. The geometries of the 2024-T351 aluminium alloy plate and the blunt projectile [19]

Table 1. Test numbers and the four respective thicknesses of 2024-T351 aluminium alloy plates [19]

Test numbers of series	Thickness of plate (mm)
A1 to A12	2.00
B1 to B9	4.00
C1 to C11	4.28
D1 to D12	8.00

Table 2. Parameters of the rigid blunt projectile [19]

Geometry	Diameter (mm)	Length (mm)
Cylindrical solid of blunt projectile	12.66	50.56

A full three-dimensional model of rigid blunt cylindrical projectile together with the 2024-T351 aluminium alloy plate were modelled by using LS-PREPOST numerical simulation software. The projectile was modelled by utilizing 2,550 rigid elements and the target plate was modelled by using 993,270 deformable constant stress solid elements. To replicate the clamping mechanism around the circumference of the circular plate; \*BOUNDARY SPC SET was used to fully clamped the circumferential edges of the target plate in the x, y and z translational and in the x, y, z rotational directions. \*CONTACT AUTOMATIC SINGLE SURFACE was employed to introduce the contact properties when impact phenomenon occurred i.e. when the projectile impacted the target plate. The respective initial velocity of the projectile just before it impacted the target plate was assigned by using the \*INITIAL VELOCITY GENERATION command. The

projectile employed \*020 RIGID material properties where it will not undergo any deformations throughout the simulation process and the target plate was modelled with \*003 PLASTIC KINEMATIC command with its mechanical properties as shown in Table 3. All these steps were created in LS-PREPOST for a total of 44 impact events as listed in Table 1 and will be processed in LS-DYNA.

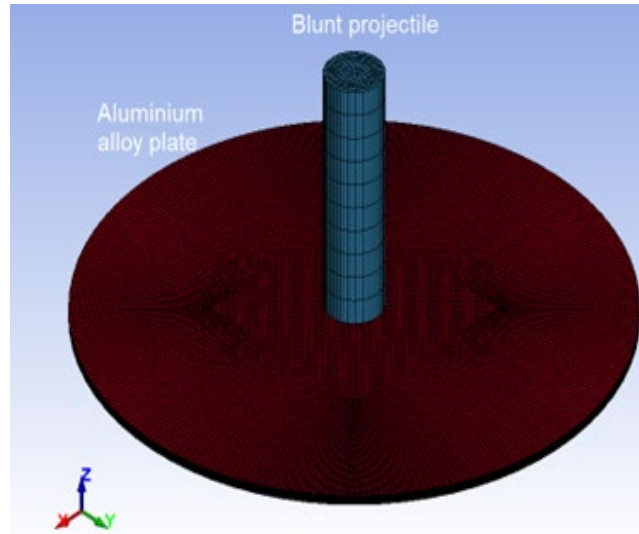


Figure 3. Three-dimensional numerical simulation models of blunt projectile (rigid elements) and aluminium alloy plate (deformable elements)

Table 3: The mechanical properties of 2024-T351 aluminium alloy plate [19]

Property	Unit	Measurement
Modulus of elasticity	$E$ (GPa)	72.00
Poisson's ratio	$\nu$	0.30
Density	$\rho$ (kg/m <sup>3</sup> )	2770.00
Yield stress constant	$A$ (MPa)	360.30
Strain hardening constant	$B$ (MPa)	649.40
	$n$	0.68
	$Q$ (MPa)	235.90
	$\beta$	8.988
	$\alpha$	0.104
Strain rate constant	$C$	0.0146
Thermal softening constant 1	$p$	1.702
Thermal softening constant 2	$m$	2.769
Reference strain rate	$\dot{\epsilon}_0^*$ (1/s)	$8.33 \times 10^{-4}$
Room temperature	$T_0$ (K)	293.00
Melting temperature	$T_m$ (K)	755.00
Inelastic heat fraction	$X$	0.90
Specific heat	$C_p$ (J / kg · K)	875.00
JC fracture criterion constants	$D_1$	0.034
	$D_2$	0.664
	$D_3$	-1.50
	$D_4$	0.011
	$D_5$	9.958
	$D_6$	3.289
MMC constants	$K$ (MPa)	678.70
	$n$	0.138
	$C_1$	0.104
	$C_2$	335.60
	$c_\theta^c$	1.00
	$c_\theta^5$	1.036



### 3.0 RESULTS AND DISCUSSION

The primary aim of this investigation is to produce reliable numerical simulation analyses predictions of blunt cylindrical projectile impacting against the 2024-T351 aluminium alloy plate and utilizing the performed experimental tests data [19] to validate on the accuracy of the numerical simulation analyses results. The numerical simulations results will be presented in two main categories, i.e. the photographs of deformations of the target plate upon impact and in terms of numerical percentages of the predicted residual velocities and deformations patterns as produced by LS-DYNA.

#### 3.1 Photographs of Target Plate Deformations

As reported in Table 1, 44 numerical simulation analyses consisting of Test series of As, Bs, Cs and Ds of the blunt cylindrical projectile impacting against the 2024-T351 aluminum alloy plate were modeled and post-processed in this study. Selected numerical simulation tests pictures are presented in this section and compared directly with the performed experimental tests [19] for comparisons and validation purposes. Figure 4 shows the predicted outputs for four different thicknesses of the target plates (in a cross-sectional view) that occurred in the central part of the target plate. It could be observed that perforations occurred in the central portion of the target plates i.e. for Test numbers A2, B7 and C3 while for Test D8; only penetration cavity was discovered in the central portion of the target plate around 50.00 % of thickness height from the bottom part of the target plate with a small amount of scabbing occurred at the top 20.00 % thickness height from the bottom part of the target plate. The predicted numerical simulation deformations outputs in Figure 4 are then compared with the performed experimental tests data deformations outputs [19] as in Figure 5 for validations purposes. It could be observed that the predicted numerical simulations deformations outputs were in good agreement with the experimental tests data outputs for three target plate thicknesses i.e. 2.00 mm, 4.00 mm and 4.82 mm but for the final target plate thickness of 8.00 mm, the predicted numerical simulation outputs showed that the target plate endured penetration process whereby the experimental test showed that it experienced perforation process.

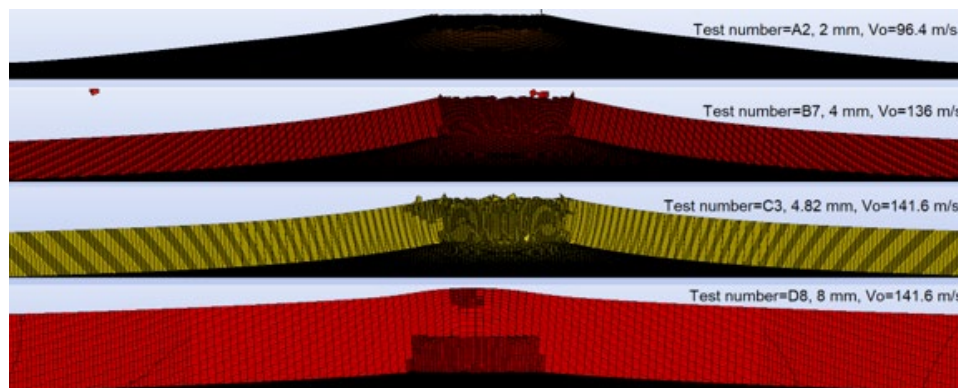


Figure 4. Plastic deformations of the 2024-T351 aluminum alloy plates as produced by the numerical simulations

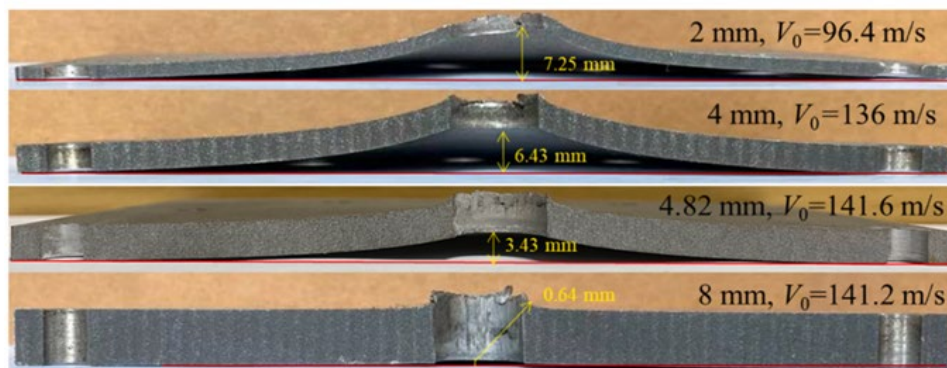
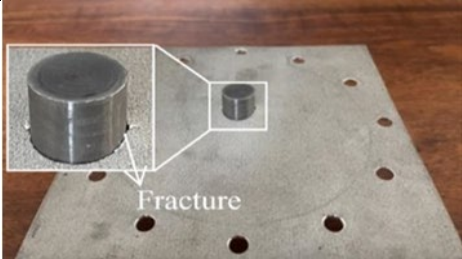
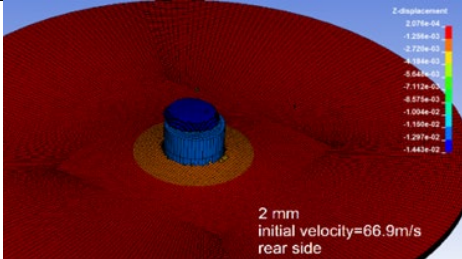
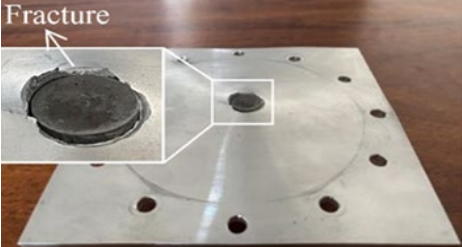
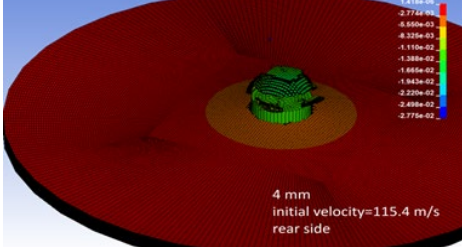
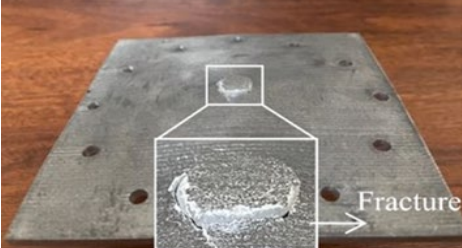
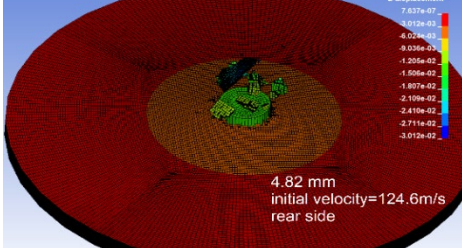
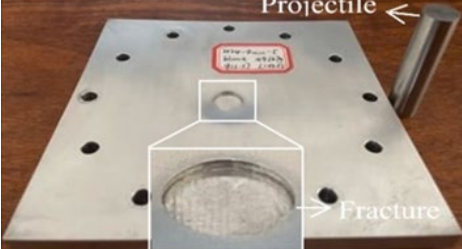
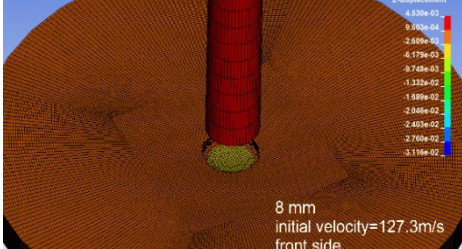


Figure 5. Plastic vertical deflections of the initial impact surfaces between the solid circular bullets and the 2024-T351 aluminum alloy plates obtained from the published experimental tests [19]

Table 4 displays another set of selected isometric view of three dimensional models of numerical simulation analyses consisting of Test series of As, Bs, Cs and Ds of the blunt cylindrical projectile impacting against the 2024-T351 aluminum alloy plate positioned along the right column compared against the published experimental tests outputs [19] located in the middle column. It could be seen that the numerical simulations results had managed to produce good agreement with respect to the experimental tests data for Test numbers A10, B6, C3, where the failure was due to the perforations of the target plate that occurred for all three tests. Furthermore, the numerical simulation prediction of test number D5 also was in good agreement with the performed experimental tests data where penetration of the target plate of around 50.00 % of the target plate's thickness height could be observed.

Table 3. Published experimental tests data of failure patterns for selected bullet and target plate impact events compared against numerical simulation predictions by LS- DYNA [19]

Test number: Plate thickness: Initial velocity: Viewing side:	Published experimental tests data [19]	Numerical simulation results predicted by LS-DYNA
A10 2 mm 66.9 m/s Rear side		
B3 4 mm 115.4 m/s Rear side		
C6 4.82 mm 124.4 m/s Rear side		
D5 8 mm 127.3 m/s Front side		

### 3.2 Residual Velocities and Deformation Patterns (Numerical Comparisons)

Table 5, Table 6, Table 7 and Table 8 show the 44 numerical simulation analyses predictions of blunt cylindrical projectile impacting the 2024-T351 aluminum alloy plate (highlighting the predicted residual velocities and predicted deformations patterns in terms of numerical accuracy) compared against the performed experimental tests data [1]. Table 5 shows the predicted residual velocities and the predicted physical deformations status of the 12 numerical simulations' results of blunt cylindrical projectile impacting against the '2.00' mm in thickness of 2024-T351 aluminum alloy plate. It could be seen that the

predicted numerical simulations' results managed to give good agreement for both percentage differences in residual velocities (with an overall average of 3.50 %) and the percentage differences of deformations status (with an overall average of 16.70 %). Table 6 displays 9 numerical simulations predicted results of blunt cylindrical projectile impacting against the '4.00' mm in thickness of 2024-T351 aluminum alloy plate.

Table 4. Residual velocity and physical deformation status of bullet impact against 2 mm thickness 2024-T351 aluminium alloy target plate as predicted by LS DYNA compared to published experimental [19]

Test No.	Initial velocity, $V_0$ (m/s)	Residual velocity, $V_r$ (m/s)	Residual velocity (m/s) by LS-DYNA	% differences of residual velocities	Physical deformation status from published experimental tests	Physical deformation status by LS-DYNA	% differences of deformation
A1	103.9	79.6	77.7	2.39 %	Perforated	Perforated	0 %
A2	96.4	65.0	63.1	2.92 %	Perforated	Perforated	0 %
A3	69.1	0.0	0.0	0.0 %	Projectile got stuck	Perforated, stuck in the plate	0 %
A4	74.3	20.4	19.8	2.94 %	Perforated	Perforated, stuck in the plate	50 %
A5	79.7	36.4	27.3	25 %	Perforated	Perforated, stuck in the plate	50 %
A6	89.1	53.0	53.5	0.94 %	Perforated	Perforated	0 %
A7	110.5	90.1	86.0	4.55 %	Projectile got stuck	Perforated	50%
A8	64.4	0.0	0.0	0 %	Projectile got stuck	Perforated, stuck in the plate	0 %
A9	125.4	103.7	107	3.18 %	Perforated	Perforated	0 %
A10	66.9	0.0	0.0	0 %	Projectile got stuck	Perforated, stuck in the plate	0 %
A11	43.1	0.0	0.0	0 %	Indentation, rebound	Indentation, rebounded	0 %
A12	55.0	0.0	0.0	0 %	Indentation, rebound	Perforated, rebounded	50 %
Total average percentage differences of residual velocities for Test A1 to Test A12 as predicted by LS-DYNA				3.5 %	Total average percentage differences of deformation status for Test A1 to Test A12 as predicted by LS-DYNA		16.7 %

Table 5: Residual velocity and physical deformation status of bullet impact against 4 mm thickness 2024-T351 aluminium alloy target plate as predicted by LS DYNA compared to published experimental [19]

Test No.	Initial velocity, $V_0$ (m/s)	Residual velocity, $V_r$ (m/s)	Residual velocity (m/s) by LS-DYNA	% differences of residual velocities	Physical deformation status from published experimental tests	Physical deformation status by LS-DYNA	% differences of deformation
B1	30.4	0.0	0.0	0 %	Indentation, rebound	Indentation, rebound	0 %
B2	104.2	0.0	0.0	0 %	Indentation, rebound	Perforated, stuck	100 %
B3	115.4	0.0	0.0	0 %	Projectile got stuck	Perforated, stuck	0 %
B4	244.5	227.7	222	2.5 %	Perforated	Perforated	0 %
B5	201.5	184.8	168	9.1 %	Perforated	Perforated	0 %
B6	117.2	20.9	29.6	41.6 %	Perforated	Perforated, moved downward slowly	50 %
B7	136.0	79.7	78.4	1.63 %	Perforated	Perforated	0 %
B8	137.3	86.3	79.5	7.87 %	Perforated	Perforated	0 %
B9	163.2	139.9	122	12.79 %	Perforated	Perforated	0 %
Total average percentage differences of residual velocities for Test B1 to Test B9 as predicted by LS-DYNA				8.4 %	Total average percentage differences of deformation status for Test B1 to Test B9 as predicted by LS-DYNA		16.7 %

Positive agreements were achieved by the predicted numerical simulations' results that managed to obtain an overall average of 8.40 % differences for the residual velocities and an overall average of 16.70 % differences for the deformation status. Table 7 presents the predicted residual velocities and the predicted physical deformations status of the 11 numerical simulations' results of blunt cylindrical projectile impacting against the '4.28' mm in thickness of 2024-T351 aluminum alloy plate. The numerical simulations had managed to provide favorable predictions outputs for two primary outputs i.e. 11.79 % of average differences for the residual velocities and 4.54 % of average differences for the deformation status. Finally, the 12 numerical simulations predicted results of blunt cylindrical projectile impacting against the '8.00' mm in thickness of 2024-T351 aluminum alloy plate are as shown in Table 8.

**Table 6. Residual velocity and physical deformation status of bullet impact against 4.28 mm thickness 2024-T351 aluminium alloy target plate as predicted by LS DYNA compared to published experimental [19]**

Test No.	Initial velocity, $V_0$ (m/s)	Residual velocity, $V_r$ (m/s)	Residual velocity (m/s) by LS-DYNA	% differences of residual velocities	Physical deformation status from published experimental tests	Physical deformation status by LS-DYNA	% differences of deformation
C1	179.4	157.8	134	15.1 %	Perforated	Perforated	0 %
C2	162.1	136.8	103	24.7 %	Perforated	Perforated	0 %
C3	141.6	102.0	56.8	44.3 %	Perforated	Perforated	0 %
C4	107.7	0.0	0	0 %	Indentation, rebounded	Indentation, rebounded	0 %
C5	115.8	0.0	0	0 %	Indentation, rebounded	Perforated, rebounded	50 %
C6	124.5	0.0	0	0 %	Projectile got stuck	Perforated, stuck	0 %
C7	198.5	183.0	156	14.8 %	Perforated	Perforated	0 %
C8	290.7	284.4	267	6.11 %	Perforated	Perforated	0 %
C9	201.2	175.2	165	5.82 %	Perforated	Perforated	0 %
C10	191.0	165.7	148	10.68 %	Perforated	Perforated	0 %
C11	240.0	226.5	208	8.17 %	Perforated	Perforated	0 %
Total average percentage differences of residual velocities for Test C1 to Test C11 as predicted by LS-DYNA				11.79 %	Total average percentage differences of deformation status for Test C1 to Test C11 as predicted by LS-DYNA		4.54 %

**Table 7. Residual velocity and physical deformation status of bullet impact against 8.00 mm thickness 2024-T351 aluminium alloy target plate as predicted by LS DYNA compared published experimental [19]**

Test No.	Initial velocity, $V_0$ (m/s)	Residual velocity, $V_r$ (m/s)	Residual velocity (m/s) by LS-DYNA	% differences of residual velocities	Physical deformation status from published experimental tests	Physical deformation status by LS-DYNA	% differences of deformation
D1	170.2	118.7	34.1	71.3 %	Perforated	Perforated, stuck	50 %
D2	163.7	118.0	5.92	95 %	Perforated	Perforated, stuck	50 %
D3	141.2	62.8	37.4	40.44 %	Perforated	Indentation, rebounded	100 %
D4	113.7	0.0	0	0 %	Indentation, rebound	Indentation, rebounded	0 %
D5	127.3	0.0	0	0 %	Indentation, rebound	Indentation, rebounded	0 %
D6	125.1	0.0	0	0 %	Indentation, rebound	Indentation, rebounded	0 %
D7	146.0	78.2	0	100 %	Perforated	Indentation, rebounded	100 %
D8	141.6	75.9	0	100 %	Perforated	Indentation, rebounded	100 %
D9	118.8	0.0	0	0 %	Indentation, rebound	Indentation, rebounded	0 %
D10	227.6	194.9	151	22.5 %	Perforated	Perforated	0 %
D11	248.6	201.5	185	8.18 %	Perforated	Perforated	0 %
D12	130.1	0.0	0	0 %	Indentation, rebound	Indentation, rebounded	0 %
Total average percentage differences of residual velocities for Test D1 to Test D12 as predicted by LS-DYNA				36.45 %	Total average percentage differences of deformation status for Test D1 to Test D12 as predicted by LS-DYNA		33 %



In reference with the good agreements that were achieved by the numerical simulations' predictions for the plate thicknesses of 2.00 mm, 4.00 mm and 4.28 mm (see Table 5, Table 6, and Table 7); the numerical simulations' predictions for the plate thickness of 8.00 mm produced larger average differences for both outputs; the average residual velocities at 36.45 % and the average differences for deformation status at 33.00 % as in Table 8.

#### 4.0 CONCLUSIONS

This current study employed numerical simulation analyses to forecast the remaining velocities of the projectile and assess the physical deformations of the target plate. A three-dimensional blunt cylindrical projectile with varying initial velocities impacted the central region of a 2024-T351 aluminium alloy plate. This plate had thicknesses of 2.00 mm, 4.00 mm, 4.28 mm, and 8.00 mm. The simulations were conducted using LS-DYNA. In conclusion, the numerical simulation analyses successfully yielded accurate predictions for the residual velocities of the projectile and the physical deformations of the target plate for the first three plate thicknesses (2.00 mm, 4.00 mm, and 4.28 mm), with discrepancies of approximately 10.00 % in all three categories. However, there were slightly larger discrepancies, around 30.00 %, for both categories when analysing the target plate with a thickness of 8.00 mm.

#### 5.0 CONFLICT OF INTEREST

The authors declare no conflicts of interest.

#### 6.0 AUTHORS CONTRIBUTION

Othman, M. Z. (Conceptualisation; Methodology; Validation; Formal analysis; Investigation; Writing - original draft)

Tan, K. S. (Formal analysis; Investigation)

Ab Ghani, A. R. (Project Administration)

#### 7.0 ACKNOWLEDGEMENTS

The authors fully acknowledged Ministry of Higher Education (MOHE) and National Defence University of Malaysia (NDUM) for their support in making this research feasible.

#### List of Reference

- [1] Espeseth, V., Børvik, T., & Hopperstad, O. S. (2022). Aluminium plates with geometrical defects subjected to low-velocity impact: Experiments and simulations. *International Journal of Impact Engineering*, 167, 104261.
- [2] Niu, Z., Liu, G., Li, T., & Ji, S. (2022). Effect of high pressure die casting on the castability, defects and mechanical properties of aluminium alloys in extra-large thin-wall castings. *Journal of Materials Processing Technology*, 303, 117525.
- [3] Jolly, M., & Katgerman, L. (2022). Modelling of defects in aluminium cast products. *Progress in materials science*, 123, 100824.
- [4] Pooppally, T. J., & Lohchab, D. S. (2024). Analysis of bullet impact test on aluminum alloy plates at varying thickness and velocities. *Materials Today: Proceedings*.
- [5] Panwar, K. S., Johri, N., Kandpal, B. C., & Singh, L. K. (2023). Analyzing ballistic impact of bullet over laminated test specimen. *Materials Today: Proceedings*, 73, 128-133.
- [6] Alwan, F. H. A., Prabowo, A. R., Muttaqie, T., Muhayat, N., Ridwan, R., & Laksono, F. B. (2022). Assessment of ballistic impact damage on aluminum and magnesium alloys against high velocity bullets by dynamic FE simulations. *Journal of the Mechanical Behavior of Materials*, 31(1), 595-616.
- [7] Børvik, T., Olovsson, L., Dey, S. *et al.*, "Normal and oblique impact of small arms bullets on AA6082-T4 aluminium protective plates," *International Journal of Impact Engineering*, Vol. 38, No. 7, 2011, pp. 577-589.
- [8] Gao, Y., Shi, L., Li, Z., Jia, Z., & Ge, Y. (2025). Macro/micro failure mechanism of transparent armour subjected to multiple impacts of 7.62 mm bullets. *Thin-Walled Structures*, 207, 112754.
- [9] Dewangan, M. K., Kumar, D., Bhardwaj, V., Manjeet, Lal, S., Sharma, P., & Kumari, R. (2022, August). Perforation of AA-2024 aluminium targets subjected to impact by spherical aluminium projectiles.

- In International Symposium on Plasticity and Impact Mechanics (pp. 473-483)*. Singapore: Springer Nature Singapore.
- [10] Stergiou, T., Baxevanakis, K. P., Roy, A., Voronov, L. V., Sazhenkov, N. A., Nikhamkin, M. S., & Silberschmidt, V. V. (2023). Mechanics of ballistic impact with non-axisymmetric projectiles on thin aluminium targets. *Part I: Failure mechanisms. Engineering Failure Analysis, 150*, 107152.
  - [11] Jafaraghaei, Y., Yu, T., & Bui, T. Q. (2022). Peridynamics simulation of impact failure in glass plates. *Theoretical and Applied Fracture Mechanics, 121*, 103424.
  - [12] Isiet, M., Mišković, I., & Mišković, S. (2021). Review of peridynamic modelling of material failure and damage due to impact. *International Journal of Impact Engineering, 147*, 103740.
  - [13] Zheng, J., Shen, F., Gu, X., & Zhang, Q. (2022). Simulating failure behavior of reinforced concrete T-beam under impact loading by using peridynamics. *International Journal of Impact Engineering, 165*, 104231.
  - [14] Yuan, R., Wen, Y., Nie, W., Liu, D., Shen, Z., & Xu, H. (2024). Dynamic response of armor-piercing bullets to blunt and penetration with protective gelatin. *Theoretical and Applied Mechanics Letters, 14*(4), 100548.
  - [15] Dhavale, O. V., Kundurti, S. C., & Sharma, A. (2024). Ballistic response of additively manufactured AA6061/AA7075 multistack plate for armor-piercing projectile. *Materials Today: Proceedings, 98*, 194-199.
  - [16] Cheng, Y. H., Wu, H., Jiang, P. F., & Fang, Q. (2023). Ballistic resistance of high-strength armor steel against ogive-nosed projectile impact. *Thin-Walled Structures, 183*, 110350.
  - [17] Elveli, B. S., Berstad, T., Børvik, T., & Aune, V. (2023). Performance of thin blast-loaded steel plates after ballistic impact from small-arms projectiles. *International Journal of Impact Engineering, 173*, 104437.
  - [18] Çelik, E., & Koç, A. (2023). Analysis of free-fall bullet injury potential in the cranium via finite elements method. *Journal of forensic and legal medicine, 97*, 102552.
  - [19] Han, J., Shi, Y., Ma, Q., Vershinin, V. V., Chen, X., Xiao, X., & Jia, B. (2022). Experimental and numerical investigation on the ballistic resistance of 2024-T351 aluminum alloy plates with various thicknesses struck by blunt projectiles. *International Journal of Impact Engineering, 163*, 104182.